Validation of a nested OGCM for the Northwest Atlantic waters

Mads Hvid Ribergaard[1]*
Anne Britt Sandø[2]

[1] *Danish Meteorological Institute, Lyngbyvej 100, DK-2100 Copenhagen, Denmark. mhri@dmi.dk*
[2] *Nansen Environmental and Remote Sensing Center, Edvard Griegsvei 3a, N-5037 Solheimsviken, Norway. annebrit@nrsc.no*

Abstract

A global Ocean General Circulation Model (OGCM), Miami Isopycnic Coordinate Ocean Model (MICOM), is used to simulate the hydrographic for the period 1948–2001 using NCAR/NCEP forcing. Increased spatial resolution of about 20–25 km is obtained by a one-way nested version of the model for the North Atlantic. We focus our study on the Northwest Atlantic sector, the Irminger Basin, the Denmark Strait and the region off Southwest Greenland.

Surface currents are generally well placed in the model, but the East Greenland Current (EGC) is significantly too weak. In contrast the Irminger Water component of the EGC has higher velocities and is found further offshore than observed from surface drifters drogued at 15 m. Surface currents are generally underestimated in the model as they are taken as the vertical mean of the mixed layer, which can be several hundred meters during winter.

Harmonic analysis is made on the monthly average fields in order to test the model variations on annual timescales. The modelled advection time from the Icelandic shelf south of Denmark Strait to Southwest Greenland within the Irminger Current is found to be on the order of a month based on the annual phase of model temperatures.

Transport of multi-year-ice east of Greenland is underrepresented in the model resulting in too warm and saline conditions off West Greenland. This further affects the baroclinic currents, especially around southeast and southwest Greenland.

Deep convection in the Labrador Sea is overestimated in the model, caused by too small extension of the west-ice in the Labrador Sea. This amplifies the Irminger Water transport into the Labrador Sea.

Keywords: OGCM; oceanography; sea-ice; deep convection; harmonic analysis; Irminger Current; East Greenland Current.

---

* Corresponding author. Tel: +45 39157207, Fax: +45 39270684

1. Introduction

A regional nested version of a global Ocean General Circulation Model (OGCM), Miami Isopycnic Coordinate Ocean Model (MICOM) has run for the period 1948–2001 using daily reanalysis forcing. Hátún et al. (2004) has validated the same model using observations in the Faroe-Shetland inflow waters. In that area, the model seems to reproduce well the seasonal and decadal temperature variability observed in the past 50 years.

The model has been used to simulate the transport of cod larvae from the Icelandic spawning grounds towards Greenland with surprising results (Ribergaard and Sandø, 2004, in prep.). They did not find a strong relation between the recruitment from the Icelandic spawning grounds and the exceptional strong year-classes of cod at West Greenland which was expected. We therefore find it necessary to validate the model performance for the Northwest Atlantic region with special focus on the surface currents in the Irminger Basin, the Denmark Strait and off Southwest Greenland.

2. Model, data and methods

2.1. Model description

The model system applied in this study is the Ocean General Circulation Model (OGCM) MICOM (Bleck et al., 1992), fully coupled to a sea-ice module consisting of the Hibler (1979) rheology in the implementation of Harder (1996), and the thermodynamics of Drange and Simonsen (1996). It is a combination of a single-layer model of the oceanic mixed layer, based on a simple closure of the turbulent kinetic energy equation (Gaspar, 1988) and a three-dimensional isopycnic coordinate model of the stratified oceanic interior. The mixed layer (ML) has temporal and spatial varying density, while the interior layers have fixed potential densities. The specified potential densities of the sub-surface layers were chosen to ensure a realistic representation of the major water masses in the North Atlantic-Nordic Sea region (Furevik et al., 2002). In the isopycnic layers below the ML, temperature and layer thickness are the prognostic variables, whereas salinity is diagnostically determined by means of the simplified equation of state (Freidrich and Levitus, 1972). The model used here offers some advantages over conventional Cartesian coordinate models with regard to depicting subduction and thermohaline ventilation processes since the depth of the ML is unambiguously defined at all times at every horizontal grid point. This allows us to draw a clear distinction between ML and interior water.

The model solves the primitive equations consisting of the momentum equation for the velocity vector, the continuity equation for mass conservation or in the isopycnic framework, for layer thickness, two conservation equations for heat and salt and the hydrostatic equation relating pressure to depth (Bleck and Boudra, 1986; Bleck et al., 1989; Bleck and Smith, 1990; Bleck et al., 1992; McDougall and Dewar, 1998).

In the horizontal, the model is configured with a local orthogonal grid mesh with one pole over North America and one pole over central Europe (Bentsen et al., 1999), which gives a horizontal resolution of 20–25 km in the Nordic Seas. Velocity and mass field variables are staggered horizontally such that u and v grid points are positioned halfway between mass grid points in x and y directions, respectively. This

is known as the Arakawa C grid. The velocity vector and the thermodynamic variables are treated as layer variables that are vertically constant within layers but change discontinuously across layer interfaces.

The bathymetry is interpolated from the ETOPO5 data base (Data Announcement 88-MGG-02, Digital relief of the Surface of the Earth, NOAA, National Geophysical Data Center, Boulder, Colorado, 1988). It is corrected and adjusted in areas of special interest and importance such as in the Gibraltar Strait and at the Greenland-Scotland Ridge to ensure that the dense water masses are able to exit at the right depths.

In the regional model, the ML temperature and salinity fields are relaxed towards the monthly mean climatological values of Levitus and Boyer (1994) and Levitus et al. (1994). The final surface heat flux, Q_{tot}, with relaxation to observed temperature T^* is expressed as

$$Q_{tot} = Q_{atm} - \lambda_T \left(T^* - T \right)$$

with

$$\lambda_T = c_p \frac{h}{t_{relax}} \rho$$

where $c_p = 3987$ J kg^{-1}K^{-1} is the specific heat of sea water, h (m) is the ML thickness, and t_relax (s) is the time scale for relaxation. The e-folding relaxation time scale is set to 30 days for a 50 m thick ML and the relaxation is reduced linearly with the ML exceeding 50 m. If the relaxation to the climatology is too strong, the model will not be able to reproduce the observed amplitude and phase shifts due to the fixed seasonal properties of the climatology. The applied relaxation is rather weak, allowing for seasonal to inter-annual variations in the simulated ML properties, as I shown in Hátún et al. (2004).

Likewise, the final surface salinity flux, S_{flux}, with relaxation to observed salinity S^* is expressed as

$$S_{flux} = S_{atm} - \lambda_S \left(S^* - S \right)$$

with

$$\lambda_S = \frac{h}{t_{relax}} \rho$$

Q_{atm} and S_{atm} are the temperature and surface salinity fluxes estimated from the atmospheric forcing fields. The surface salinity fluxes are simply estimated as the difference between evaporation and precipitation.

Daily mean NCAR/NCEP re-analysis (Kalnay et al., 1996) fresh water, heat and momentum fluxes are used to force the system by applying the schemes of Bentsen and Drange (2000). If the model sea surface state is equal to the NCAR/NCEP sea surface state, the turbulent fluxes of momentum and heat are taken from the re-analysis data. If the sea surface state differs between the ocean model and the re-analysis data, the fluxes will be modified according to the Fairall et al. (1996) scheme. In combination with the Total Runoff Integrating Pathways (TRIP) data base, these fields are also used to incorporate river runoff.

The model is initialized and nested with interpolated model data from a global version of MICOM (Furevik et al., 2002; Bentsen et al., 1999) and run for the period 1948–

2001. The data from the global model is interpolated to the nested grid with twice the resolution of the global model.

The continuity, momentum and tracer equations are discretised on an Arakawa C-grid stencil. The diffusive velocities (diffusivities divided by the size of the grid cell) for layer diffusion, momentum dissipation, and tracer dispersion are 0.015 m s^{-1}, 0.015 m s^{-1} and 0.005 m s^{-1}, respectively. The diapycnal mixing coefficient K_d (m^2 s^{-1}) is parameterized according to the Gargett (1984) expression $K_d=3 \times 10^{-7}$ / N, where N (s^{-1}) is the Brunt-Väisïlä frequency. The numerical implementation of the diapycnal mixing follows the scheme of McDougall and Dewar (1998).

The nesting approach applies a boundary relaxation scheme towards the outer (i.e. global) solution. This results in a so-called one way nesting where the boundary conditions of the regional model are relaxed towards the output from the global model. For the slowly varying baroclinic velocity, temperature, salinity and layer interface variables, this is a fully appropriate way to include the boundary conditions. For the barotropic variables, the relaxation approach requires careful tuning to avoid reflection of waves at the open boundaries. The regional model reads the global fields once a week and interpolates in time to specify the relaxation boundary conditions at each time step.

2.2. Climatologies

2.2.1. Surface temperature and salinity

The ¼ degree World Ocean Atlas 2001 (WOA) version 2 climatology is used for validating MICOM surface salinity and temperature. It is interpolated onto the grid used by MICOM, which has similar resolution as the WOA.

The ¼ degree WOA uses basically the same objective analysis technique as in the 1 degree WOA described in Stephens et al. (2002) for temperature and Boyer et al. (2002) salinity treatment. In the ¼ grid WOA, the objective analysis technique calculates the mean field by a weighted difference between the gridpoint and points within a certain radius. This is done three times with decreasing radius of influence: 321 km, 267 km and 214 km. Initial guess was taken as the 1 degree WOA. Then a median smoother was applied using the nearest 5 points on either side in north–south and east–west direction and finally each point was vertically stabilized with respect to calculated density. The monthly means were further smoothed using the annual field and the first three harmonics from a Fourier analysis for each month (see http://www.nodc.noaa.gov/OC5/WOA01/qdegmethod.pdf for details).

Mixed layer depths from WOA are calculated as the shallowest depth below 20 m, where the Brunt-Vaïsälä frequency squared exceeding 2.5 10^{-6} s^{-2} corresponding roughly to a vertical density gradient of 2.5 × 10^{-4} kg m^{-3} /m or a vertical potential vorticity gradient of 30×10^{-12} m^{-1}s^{-1}/m.

For validation we also tried the 1 degree Polar Science Center hydrographic climatology (PHC) version 2.1 (Steele et al., 2001). It is similar to the widely used Levitus climatology, but refined in the Arctic. However, it turned out that its resolution was too coarse for validation of MICOM. Especially around the southern

part of Greenland the Polar Water was hard to identify in the PHC and we decided not to use it.

2.2.2. Sea-ice

For validation of the sea-ice extent in the model we use the Walsh and Chapman Northern Hemisphere Sea Ice Data Set (W&A) for January 1901 – August 1995 (Walsh, 1985, Chapman and Walsh, 1991). Monthly mean sea-ice extents are estimated by calculating the mean concentration and defining the ice-edge as the 15 % concentration line. Maximal annual sea ice extent is defined by the 5 % concentration line. For the model ice-edge we use the same procedure, but define the ice-edge as the 0.1 % concentration line which basically is the maximum coverage. The reason for this is that the model under predicts the extent of sea-ice.

2.2.3. Surface drifters

For direct validation of the surface currents in the model, satellite-tracked surface drifters drogued at 15 m depth are used to make a surface velocity map for the 1990s (Jakobsen et al., 2003 for details). The data are mapped in 1° latitude times 2° longitude boxes, a scale well above the internal radius of deformation, and shift the boxes by half the box size in each direction. The resolution is then about 50 km, but somewhat smoothed since the boxes overlap. This is about 2½ times coarser resolution than that of MICOM. Most of the drifters in the Icelandic waters and in the Irminger Basin are from WOCE efforts during the second half of the 1990s. The distribution of data is not homogeneous neither in time nor in space. The Lagrangian nature of the measurements contributed to the inhomogeneous data distribution. In particular, there are very few data in the East Greenland Current, especially in the Denmark Strait and further north, due to the presence of ice in this area.

In order to remove tides and eddies from each drifter track, a filter is applied with a cutoff period of 18 days (see Jakobsen et al., 2003 for details)

2.2.4. Fylla section

Timeseries of temperature and salinity from the Fylla section near 64°N off West Greenland are used for the period 1950–2003 (Ribergaard and Buch, 2004). The cruises are all performed in June/July but temperatures at the Fylla Bank st. 2 are corrected for seasonality to represent mid-June.

3. Results and discussion

3.1. Surface currents

The mean surface velocity from MICOM and the mean 15 m velocities deduced from satellite-tracked surface drifters are shown in Figure 1. The main branches are highly steered by the topography both in the model and in the drifter climatology as stated by e.g. Jakobsen et al., 2003 for the latter case. The Irminger Current (IC) is topographically guided anticlockwice in the Iceland Basin. It crosses the Reykjaness Ridge at about 57–60°N and continues anticlockwice in the Irminger Basin.

South of the Denmark Strait the IC splits into two branches. The main branch continues towards Greenland and is easily recognized in both MICOM and the drifter climatology. The second branch crosses Denmark Strait but it is hard to locate exactly where the branching is taking place both in the model and in the drifter climatology. However, it appears to be quite similar in magnitude and almost identical in direction, except for the outer part of the southwest Icelandic shelf, where the currents are directed towards shallower depths in MICOM and not following the topography as in the drifter climatology.

The East Greenland Current (EGC) passes Denmark Strait from the north along the East Greenland coast. Due to sea-ice, this current is clearly underrepresented in the drifter climatology, especially north of the Denmark Strait. In the strait the front between the IC and the southward EGC is sharp in the climatology and especially in the model due to its higher spatial resolution.

Both the EGC and the West Greenland Current (WGC) are wider and much weaker in MICOM compared to the drifter climatology. Especially the Polar Water component of the EGC is much weaker and the WGC seems to be absent close to the coast in MICOM. Also a major part of the IW seems to diffuse into the interior of the Labrador Sea between 60°N and 62°N. In the drifter climatology the WGC is more confined to the shelf until 63°N–64°N where it turns towards the Canadian side.

The weak MICOM current velocities around Greenland can have several reasons. It is well known, that models do underestimate strong currents simply because of their horizontal resolution. Secondly MICOM does not have a surface Ekman layer. The wider surface layer is simply the surface mixed layer, which can be quite deep during winter. Thereby, the surface currents are much underestimated as the vertical mean current of the mixed layer. The mixed layer depth (MLD) is shown in Figure 6. As expected the MLD is shallowest in summertime. From June–September the MLD is usually less than 100 m and below 50 m in most areas except for the Irminger Current. In July and August the MLD is close to 20 m and less than 50 m everywhere except in the Fram Strait. In these summer months, the MICOM surface currents are expected to be most correct. However, we cannot confirm this statement, as the drifter data are too sparse and irregular spaced to make seasonal means.

By use of two CTD stations, a vessel-mounted ADCP and a thermosalinograph, Bacon et al. (2002) found, that a 15 km wide freshwater jet close to Southeast Greenland coast transports about 1 Sv (10^6 m^3/s). They argue that this jet, they call it the East Greenland Coastal Current (EGCC), is forced by continuous runoff by meltwater and precipitation from Greenland. It is therefore expected, that this current has a strong seasonality. However, in MICOM there is no sign of such a coastal current, but the resolution of about 20 km is probably too coarse to reproduce it correctly.

3.2. Surface temperature, salinity and sea-ice

In Figure 2 the annual mean surface salinity, temperature and density are shown for MICOM and WOA. For WOA the surface is defined as 0–20 m, whereas for MICOM

the surface layer is equal to the mixed layer depth which undergoes large annual and spatial variations mainly due to cooling in winter time (Figure 6a). The minimum mixed layer depth in the model is 20 m and the maximum depth is about 3 km.

The front around the southern part of Greenland between the Polar Water and the Irminger Water is much weaker in MICOM than in WOA, especially in temperature but also in salinity. This can be linked to the sea-ice distribution in the model (Figure 2 and Figure 3). In both the Labrador Sea/Davis Strait and more pronounced in the Irminger Basin/Denmark Strait, the model temperature front is right at the ice edge, which is evident in the monthly data. Simulations of the multi-year-ice entering the Greenland Waters through the Fram Strait is transported too short a distance before it melts, compared to sea-ice observations (Figure 2 and Figure 3). Normally it rounds Cape Farewell from around January to July and has its northernmost position on the west coast at about Paamiut (Frederikshaab) at 62°N. Both the position and the timing can vary substantially from year to year and on longer timescales (e.g. Buch, 2000; Schmith and Hansen, 2003). In contrast, the sea-ice in MICOM never rounds Cape Farewell in any month, and the maximal extent is around 62°N at the east coast (Figure 3). In fact, the sea-ice concentration is highly underestimated almost all along the East Greenland Coast for every month of the year with the exception of December–April, where MICOM overestimates the sea-ice concentration just north of Denmark Strait.

A careful examine of the model code reveals, that the reason for the underestimation of sea-ice in the model stems from problems with the nesting of the ice-velocities. The fluxes at the boundaries are therefore almost non-existing and the sea-ice represented in the nested model is only first-year ice generated by the sea-ice module.

On the East Greenland shelf north of Denmark Strait, the MICOM temperatures are slightly too high while the salinities are much too high by more than 0.5. On the East Greenland shelf south of Denmark Strait, both the surface salinity and the temperature are highly dependent on the ice-edge. In areas covered by sea-ice in the model south of the Denmark Strait, the model salinity and temperature are generally too low, and opposite for areas not covered by sea-ice. This is likely connected to the different position of the ice edge, which is much more retreated in MICOM. This changes the position of the front between the warm and saline Irminger Water and the cold and low-saline Polar Water. Thereby, the sign of MICOM minus WOA temperature and salinity alter close to the ice-edge.

On the South West Greenland shelf, both salinity and temperature are much too high in the model by about 0.5–1 and 1.5–2°C, respectively. As the multi-year ice in the model is absent, the surface waters will not continuously be diluted by melting of sea ice, but will only by runoff from land. This explains the high MICOM temperatures and salinities south and southwest of Greenland. Indeed, this holds all year around in the monthly fields. The net result of the high salinities and temperatures is a decrease in the horizontal density gradient, and thereby a decrease in the baroclinic velocities. On the ice-free side of the ice-edge off Southwest Greenland, the low-saline and cold Polar Water become lighter as it is heated during summer and the modelled currents become too weak, as the cross-current pressure gradient decrease. On the contrary, the gradient between the Irminger Water and the heated Polar Water increases and a jet is formed.

Over the deeper parts of the Labrador Sea, Irminger Basin and Iceland Basin the model surface salinities are too low by 0–0.2 and the surface temperature too low by 0.5–2.0°C. In the Baffin Bay and on the Canadian shelf the model temperatures are generally too low by 0.5–1.5°C but the salinities are much too high by 0.3–0.5 and even more in large areas.

Both on the East Greenland shelf and in Baffin Bay observations are sparse in time and space, but the model certainly has a bias in both areas, which at least for temperature can be linked to the low sea-ice concentration in the model as seen in Figure 3. The underrepresentation of sea-ice is most obvious on the east coast of Greenland. Major parts of this sea-ice are formed in the Arctic Ocean several years earlier (called multi-year-ice) and transported through Fram Strait. In contrast most of the ice in Baffin Bay (called west-ice) is one-year ice formed locally, and is therefore not as much influenced by advection of water masses.

3.3. Annual variations in the surface hydrography and sea-ice

From the previous section it is clear, that MICOM has an offset in both surface temperature and salinity in parts of the Northwest Atlantic Waters. Here we investigate if the variations in the model are similar to observations on annual and shorter timescales. A harmonic analysis is performed both on the monthly mean climatologies and on the MICOM monthly mean surface fields for the period 1948–2001 (Figure 4a–b).

Generally, most of the variance is explained by the annual harmonics both for salinity and temperature. For salinity, some areas are less well explained by the annual harmonics but better by the semi-annual harmonics. However, in these areas the variations are small and the harmonic analysis gives no meaning as just minor noise can disturb the phase of maximum. For temperature, the areas partly covered by sea-ice have a significant semi-annual component that makes the resulting temperature signal constant when covered by ice and peaks when it is ice-free. This is most noticeable in the Baffin Bay, but also north of Denmark Strait in MICOM. The latter is due to the lack of sea-ice in the area during summer as seen in Figure 3 by looking at the ice-edge.

On the shelf around Greenland and Canada, where the salinity amplitude are significant, the phase maximum agrees well between MICOM and WOA. In the southern Labrador Sea, Irminger Basin and Iceland Basin the MICOM salinity generally peaks a few month later than in WOA, but as the amplitudes are low in these waters, the harmonic analysis is quite uncertain here. Therefore we find, that the annual phase for maximum salinity agrees well between the MICOM and WOA. In contrast, the phase for maximum temperature differs quite a lot between MICOM and WOA. Compared to WOA, the maximum temperature in MICOM in mid-August is about one month to early in the southern parts of the Labrador Sea, Irminger Basin and the Iceland Basin.

One striking behaviour of MICOM is seen in the phase for maximum temperature. In MICOM, the Irminger Water is easily followed from the Denmark Strait to the Labrador Sea as a lagged maximum phase that increases by about a month as it

approaches the Labrador Sea. This clearly reflects the advective timescale of Irminger Water in the model. Such advective features are not seen in the WOA but instead the phase map looks much more unstructured. We believe the lack of structure in the WOA is somehow misleading and mainly caused by the relative few and unequally spaced data available for constructing monthly average fields, but also by the averaging procedure used for the climatology. However, as the Irminger Water rounds Cape Farewell it should not be visible any more, as it subducts below the Polar Water in the West Greenland Current (Pickart et al., 2003b).

The absolute differences of the MICOM minus WOA annual amplitudes of salinity and temperature are shown in Figure 5 (middle). The amplitude of the annual variations for surface salinity agrees quite well for the open water in the Iceland Basin, the Irminger Basin and in the Labrador Sea. For temperature, the annual variations agree within 1°C in the same area. In contrast, on the shelves around Greenland and East Canada MICOM underestimates the annual variations in salinity and overestimates the temperature variations. On the shelf off East Greenland and off West Greenland south of Disko Bay (68°N) the annual variations of salinity are underestimated by 0.25–1 and temperature variations are overestimated by 0.5 –2°C and even above 4°C south of Denmark Strait. Similar, but smaller differences are seen on the shelf on the Canadian side of the Labrador Sea. In the Baffin Bay the salinity variations are up to 1 on the Canadian side, whereas the temperature variations are similar in MICOM and WOA.

The additional temperature variations on the shelves off southeast and southwest Greenland in MICOM clearly reflects the under-representation of multi-year-ice as previously discussed. The low salinity variations are less obvious, but could be a result of too much mixing in the model and/or too little run-off from the Greenland ice-cap. Similarly, on the Canadian side, the coverage of one-year-ice is underestimated in MICOM, and therefore higher temperature variations are expected. The differences in Baffin Bay are not clear, but they could partly be caused by a poor climatology, as the observations in this area are extremely sparse both in time and space.

3.4. Mixed layer depth and deep convection

Deep water formation by open ocean deep convection, which is one of the driving mechanisms for the Atlantic meridional overturning circulation, is restricted to a small number of sites. In the North Atlantic Ocean, the Greenland Sea and the Labrador Sea are known as the most important sites, but recently Pickart et al. (2003b) showed that deep water formation also takes place in the southern part of the Irminger Basin contributing to the mid-depth Atlantic Water.

During winter, cold polar air masses blows off the Canadian land mass as storms pass by, removing heat over a large portion of the Labrador Sea. This heat loss is strong enough for deep water formation to take place. As the surface salinities are quite high, the generally cyclonic circulation lifts the isopycnals so ventilation of deeper water can take place, and the water masses become close to neutral buoyancy. In the southern Irminger Basin the mechanism for buoyancy loss is quite different (Pickart et al., 2003a). Here the Greenland continent acts as a wall for the weather systems and

consequently, a jet (the Greenland tip jet) forms periodically as low pressure systems passes by (Doyle, 1999; Cappelen et al., 2001). This jet is associated with high heat flux and strong wind stress curl over a limited area (Pickart et al., 2003a). Convection at both sites is positive correlated with the North Atlantic Oscillation.

The strong buoyancy loss in the Labrador Sea is well represented in the National Centers for Environmental Prediction (NCAR/NCEP) reanalysis global meteorological fields, which have a spatial resolution of 1–2.5°, whereas the heat loss in the Irminger Basin is significantly lower in NCAR/NCEP compared to observations (Pickart et al., 2003).

In MICOM the mixed layer depth (MLD) is simply the depth of the upper layer, which is forced to be at least 20 m thick. The modelled MLD is shown in Figure 6a for each month. In Figure 6b the MLD calculated from WOA are shown.

In the Labrador Sea, the deep convection in MICOM is both deeper and covers a larger horizontal area than in WOA. The deep convection is clearly linked to the extension of west-ice, so that convection takes place just east of the ice-edge as can be seen in Figure 6a–b and Figure 7. As the amount of west-ice is too small in the model, the convection takes place west of the observed convection site (Figure 7). This has at least two implications. First, the buoyancy loss is too high in the model, as the model makes convection at a location which is normally covered by sea-ice. Thereby, the heat loss in the model is calculated using NCAR/NCEP surface temperature over sea-ice, which is considerable colder than the temperatures over open water. Secondly, the distance from the North Atlantic Current to the model convection site has become slightly longer. Consequently, as buoyancy loss by cooling is continuously taking place over this distance during wintertime, the heat loss has also increased slightly.

Deep water formation in the Irminger Basin around 60°N as presented by Pickart et al. (2003) is hardly seen in MICOM. The NCAR/NCEP model is simply too coarse to reproduce the relative small scale phenomena and thereby the correct forcing.

Besides the deep convection, large areas of the Northwest Atlantic Ocean are subject to shallower convection during wintertime, which form mode waters. In MICOM this is easily seen in the core of the Irminger Current, e.g. along the Reykjaness Ridge and over water depths of 1000–2000 m in the northern rim of the Iceland Basin. Off East Greenland, the core of the Irminger Water can be tracked at relative large MLD in the Irminger Basin and south of Greenland in the Labrador Sea. In MICOM, the Irminger Water is seen as a narrow and 800–1000 m deep mixed layer, which is actually directly connected to the deep convection site in the Labrador Sea.

3.5. Transport through Denmark Strait

In Figure 10 the modelled transports through Denmark Strait are shown. We have divided the flow into four types of water masses:

- Polar Water (PW) defined by southward flow with salinities below 34.
- Polar Intermediate Water (PIW) defined by salinities above 34, densities below 27.55 kg/m^3 and southward flow.
- Irminger Water (IW) defined as northward flow.

• Denmark Strait Overflow Water (DSOW) defined by densities above 27.55 kg/m^3 and southward flow.

These definitions are much different to those normally given in the literature, but they are defined according to the water masses in the model. Generally, the salinities are too low in the whole section, while the bottom temperatures are more correctly represented. This greatly affects the properties of the DSOW, which is not as dense as observed (above 27.8 kg/m^3). The maximum mean salinities in the Denmark Strait are well below 35 and far from the salinities observed within the IW, which even north of Iceland are above 35 (Jónsson and Brien, 2003). In the model, PIW is not identifiable as a water mass with unique characteristics. Instead, it is defined by its location within the Denmark Strait section in order to give realistic estimates of the transport of PW, IW and DSOW. All together, the model results are not directly comparable with observations, but the variability could be comparable, which is investigated below.

The calculated transports through the Denmark Strait are summarized in Table 1. Note that the chosen definitions of water masses greatly affect the magnitude of the calculated transports, whereas the calculated variability is more constant.

Table 1. Modelled transport through Denmark Strait and standard variations calculated using weekly fields as well as 1-year running mean fields in order to remove annual cycles. PW= Polar Water, PIW = Polar Intermediate Water, IW = Irminger Water, DSOW = Denmark Strait Water.

Transport	PW	PIW	IW	DSOW
Weekly	-1.3 ± 0.9 Sv	-1.3 ± 0.8 Sv	0.5 ± 0.3 Sv	-3.0 ± 1.1 Sv
1 year running mean	-1.3 ± 0.5 Sv	-1.3 ± 0.3 Sv	0.5 ± 0.1 Sv	-3.0 ± 0.6 Sv

The transport of the IW seems to be very stable in magnitude but only half of the 1 Sv reported by Kristmannsson (1998), Hansen et al. (1999) and Hansen and Østerhus (2000) (Figure 10). Later this transport estimate was adjusted to 0.8 Sv (Jónsson and Breim, 2003, S. Jónsson, personal communication in Hansen et al. 2003) which is closer to the model result.

The transport of PW seems to be too low. Hansen and Østerhus (2000) estimated the total transport of PW from the Arctic Mediterranean to the North Atlantic through the Canadian Archipelago and the Denmark Strait to 3 Sv. They have no direct measurements of the transport, but estimated this value by closing the water balance for the Arctic Mediterranean. As most of the observed fresh water export from the Arctic Ocean in the surface is through the Fram Strait, the transport of 1.3 Sv within the EGC by the model seems to be too weak. We therefore believe that the high model temperatures and salinities off West Greenland are caused by a too weak EGC.

The transport of PW in the model does show large variations in the 54 years period, but the Great Salinity Anomaly in the late 1960s do not show up in the Denmark Strait. Mortensen et al. (1991) calculated the baroclinic component of the PW in the Denmark Strait for September 1987–1990 and found it highly variable between 0.6 and 2.0 Sv. This variability is similar to the variability found in the model.

The modelled transport of DSOW through Denmark Strait is about 3 Sv which is close to the 2.9 Sv estimated by Dickson and Brown (1994) using direct current

measurements and hydrographic sections. They found it to be fairly stable on seasonal and long timescales. In contrast, the model show large and permanent seasonal variations of about 1 Sv and variations of about 0.5 Sv on longer timescales. However, recent direct current observations show transport fluctuations on the overflow on the same order (R. Käse, personal communication). Observed large fluctuations of the overflow on timescales of a few days associated with meso-scale eddy activity immediately downstream of the sill are detected using direct current measurements (Smith, 1976; Dickson and Brown, 1994) and temperature and altimetry data (Høyer and Quadfasel, 2001). We are not able to detect such variability in the model, as we are using weakly current fields for validation.

The modelled transport of PIW is about 1.3 Sv. It has a long term variability of about 0.3 Sv and a persistent seasonal variability of about 1 Sv. Its long term variability is not in phase with either the PW or the DSOW transport. As this water mass is only defined in order to get realistic transports within the Denmark Strait, its variability acts as an additional uncertainty of the estimated transport of PW and DSOW.

3.6. Timeseries from the Fylla section

In Figure 8 the mean (0–40 m) salinity and potential temperature on top of Fylla Bank st. 2 are shown. The mean salinity and temperature is higher in MICOM than in observations by 0.2 and 1.2°C respectively. The variance is 4 times lower for the modelled salinity and 1.5 times higher for modelled temperature. The correlation between the model and the observations for salinity is 0.03 (0.02 for 3-years running mean), while the correlation for temperature is 0.49 (0.48 for the yearly and 3-years running mean). In other words, the model is not able to correctly reproduce the salinity variations, whereas the temperature variance is better reproduced.

The Great Salinity Anomaly in the late 1960s does neither show up in the salinity nor in the temperature in MICOM, while the two cold periods 1982–1984 and 1989–1994 are well represented. The Great Salinity Anomaly is an advective process which started in the Arctic Mediterranean by a fresh water pulse through the Fram Strait in the late 1960s (Dickson et al., 1988; Belkin et al, 1998 (and references therein)), while the two following cooling periods are both believed to be a result of local cooling (Rosenørn et al, 1985; Buch, 2000). This suggests that the air-sea exchanges are well represented in the model while the advective processes are less well represented. Both temperature and the salinity are too high in the model at West Greenland. This indicates that either the East Greenland Current and the transport of sea-ice therein are too weak or that the Irminger Current branch towards Greenland is too strong. The former chapters support the first explanation, as the sea-ice extent is too small in the model.

In Figure 9 the salinity, potential temperature and density are shown for Fylla Bank st. 4 (west of Fylla Bank on the continental slope) for four different depth intervals from the model and from observations. In the model, the salinities above 150 m (mainly Polar Water) are too high by 0.5–1 and too low by about 0.1 in the waters below 150 m (mainly modified Irminger Water). The model temperature at the upper 150 m is between 1 and 2°C too high, whereas the temperatures in the interval 150–400 m are slightly too high, and slightly too low in the interval 400–600 m. This results in too dense water above 400 m and the vertical stability in the water column is too weak. In

the model both the salinity and the temperature seems to converge to a value in between the surface and bottom values. This indicates too high vertical mixing in the model or alternatively, too weak advection velocities. Major jumps in salinities above 150 m and temperatures in the 50–150 m interval are seen in the early 1980s. Thereafter the density differences between the surface and the bottom waters are even weaker but the model drift seems to have stabilized. The reason for the drift is however unknown.

The weaker stability of the water column suggests that the vertical mixing in the model is too high and that the advection of water into the area is too weak.

The jump in salinity in the early 1980s in the model can be connected to convection in the Labrador Sea combined with a weak WGC. As dense water forms, it spreads horizontally and mixes with the surrounding waters. Thereby the bottom water in the Fylla Bank st. 4, which initially is IW or modified IW, becomes slightly less saline and the temperature decreases. Eventually, if this mixing is going on for long time, the surface waters become more saline and slightly colder. Normally, mixing from below at Fylla Bank would result in higher surface temperatures, but the weak extent of multi-year-ice in the model results in high surface temperatures, because the PW is less isolated by sea-ice and is less cooled by sea-ice melting. This mixing process is only possible as long as the advection of PW and IW within the WGC is weak.

4. Conclusions

- The modelled extent of multi-year-ice (storis) is much too low, which directly affects the temperatures at South East and West Greenland and indirectly changes the baroclinic currents.
- Surface currents are generally underestimated by the model as the surface currents are taken as the vertical mean of the mixed layer, which can be several hundreds of meters during winter.
- Velocities within the East- and West Greenland Current are much too low in the model compared to velocities derived from surface drifters. On the contrary, the Irminger Water component of the EGC has slightly higher velocities and is situated further offshore in the model.
- Convection in the Labrador Sea is deeper and located more westward in the model than observed. The latter is caused by the retreated ice-edge in the model.
- The salinity variations at Fylla Bank are poorly represented in the model, while the temperature variations are much better reproduced. In the model, there is no sign of the "Great Salinity Anomaly" in the late 1960s, but the two following cold periods in the 1980s and 1990s are easily seen. Thereby we conclude that the air-sea exchanges appear to be well represented in the model whereas the advection processes are less well represented in the Irminger Basin / Labrador Sea area.
- Modelled transport through Denmark Strait of:
  1. Irminger Water compares well to observations. It is stable but slightly lower in magnitude than reported in the literature. However, the salinity is much too low in the model.
  2. Polar Water seems to be slightly too low. The "Great Salinity Anomaly" in the late 1960s does not show up, but the variability seems to be fairly ok in amplitude.

3. Denmark Strait Overflow Water is right in magnitude in mean, but shows large variability on both seasonal and longer timescales which is in agreement with recent observations (R. Käse, personal communication). However, its density is much too low in the model caused by a combination of too low salinity and too high temperatures.

Acknowledgement

References

Bacon, S., Reverdin, G., Rigor, I.G., and Snaith, H.M., 2002. A freshwater jet on the east Greenland shelf. *Journal of Geophysical Research* **107 (C7)**, doi:10.1029/2001JC000935.

Belkin, I. M., Levitus, S., Antonov, J. and Malmberg, S. A., 1998. "Great Salinity Anomalies" in the North Atlantic. Progress in Oceanography 41, pp. 1-68.

Bentsen, M., and Drange, H., 2000. Parameterizing surface fluxes in ocean models using the NCEP/NCAR reanalysis data. In *RegClim General Technical Report* **4**, 149–158. Norwegian Institute for Air Research, Kjeller, Norway.

Bentsen, M., Evensen, G., Drange, H., and Jenkins, A.D., 1999. Coordinate transformation on a sphere using conformal mapping. *Monthly Weather Review* **127**, 2733–2740.

Bleck, R, and Smith, L.T., 1990. A wind-driven isopycnic coordinate model of the north and equatorial Atlantic Ocean. 1: Model development and supporting experiments. *Journal of Geophysical Research* **95**, 3273–3285.

Bleck, R., and Boudra, D., 1986. Wind-driven spin-up in eddy-resolving ocean models formulated in isopycnic and isobaric coordinates. *Journal of Geophysical Research* **91**, 7611–7621.

Bleck, R., Hanson, H.P., Hu. D., and Krauss, E.B., 1989. Mixed layer-thermocline interaction in a three-dimensional isopycnic coordinate model. *Journal of Physical Oceanography* **19**, 1917–1439.

Bleck, R., Rooth, C., Hu, D., and Smith, L.T., 1992. Salinity-driven thermocline transients in a wind- and thermohaline-forced isopycnic coordinate model of the North Atlantic. *Journal of Physical Oceanography* **22**, 1486–1505.

Boyer, T. P., C. Stephens, J. I. Antonov, M. E. Conkright, R. A. Locarnini, T. D. O'Brien, and H. E. Garcia, 2002, *World Ocean Atlas 2001 Volume 2: Salinit*y, S. Levitus, Ed. NOAA Atlas NESDIS 50, U. S. Government Printing Office, Washington, D. C., 176 pp.

Buch, E., 2000. Air-sea-ice conditions off Southwest Greenland 1981–1997. *Journal of Northwest Atlantic Fishery Science* **26**, 1–14.

Cappelen, J., Jorgensen, B.V., Laursen, E.V., Stannius, L.S., and Thomsen, R.S., 2001. The Observed Climate of Greenland, 1958–99, with Climatological Standard Normals, 1961–90. *DMI Technical Report* **00-18**, Danish Meteorological Institute, Copenhagen.

Chapman, W.L. and Walsh, J.E., 1991. Long-Range Prediction of Regional Sea Ice Anomalies in the Arctic. *Weather and Forecasting* **6(2)**, 271–288.'

Dickson, B., 2003. Stirring times in the Atlantic. *Nature* **424**, 141–142.

Dickson, R.R., and Brown, J., 1994. The production of North Atlantic Deep Water: Sources, rates, and pathways. *Journal of Geophysical Research* **99(C6)**, 12319–12341.

Dickson, R.R., Meincke, J., Malmberg, S.A., and Lee, A.J., 1988. The "Great Salinity Anomaly" in the Northern North Atlantic 1968-1982. *Progress in Oceanography* **20**, 103–151.

Doyle, J. D., and Shapiro, M.A., 1999. Flow response to large-scale topography: the Greenland tip jet. *Tellus* **51**, 728–748.

Drange, H., and Simonsen, K., 1996. Formulation of air-sea fluxes in the ESOP2 version of MICOM. *Technical report* **125**, Nansen Environmental and Remote Sensing Center, Norway.

Fairall, C.W., Bradley, E.F., Rogers, D.P., Edson, J.B., and Young, G.S., 1996. Bulk parameterization of air-sea fluxes for Tropical Ocean-Global Atmosphere Response Experiment. *Journal of Geophysical Research* **101**, 3747–3764.

Friedrich, H., and Levitus, S., 1972. An approximation to the equation of state for sea water, suitable for numerical ocean models. *Journal of Physical Oceanography* **2**, 514–517.

Furevik, T., Bentsen, M., Drange, H., Johannessen, J., and Korablev, A., 2002. Temporal and spatial variability of the sea surface salinity in the Nordic Seas. *Journal of Geophysical Research* **107** (C12), 8009, doi:10.1029/2001JC001118.

Gargett, A.E., 1984. Vertical eddy diffusivity in the ocean interior. *Journal of Marine Research* **42**, 359–393.

Gaspar, P., 1988. Modelling the seasonal cycle of the upper ocean. *Journal of Physical Oceanography* **18**, 161–180.

Hansen, B., and Østerhus, S., 2000. North Atlantic-Nordic Seas exchanges. *Progress in Oceanography* **45**, 109–208.

Hansen, B., Larsen, K.M.H., Østerhus, S., Turrell, B, and Jónsson, S., 1999. The Atlantic inflow to the Nordic Seas. *The International WOCE Newsletter* **35,** 33–35.

Hansen, B., Østerhus, S., Hátún, H., Kristiansen, R., and Larsen, K.M.H., 2003. The Iceland–Faroe inflow of Atlantic water to the Nordic Seas. *Progress in Oceanography* **59**, 443–474.

Harder, M., 1996. Dynamik, Rauhigkeit und Alter des Meereises in der Arctis. *Ph.D. Thesis*, Alfred-Wegner-Institut für Polar- und Meeresforschung, Bremerhaven, Germany.

Hátún, H., Sandø, A.B., Drange, H., and Bentsen, M., 2004. Seasonal to decadal temperature variations in the Faroe-Shetland inflow waters. In: *Climate variability of the Nordic Seas*, edited by Drange, H., Dokken, T., Furevik, T., Gerdes, R., and Berger, W., American Geophysical Union, Washington D.C.

Hibler, W., 1979. A dynamic thermodynamic sea ice model. *Journal of Physical Oceanography* **9**, 815–846.

Høyer, J.L., and Quadfasel, D., 2001. Detection of deep overflows with satellite altimetry. *Geophysical Research Letters* **28 (8)**, 1611–1614.

Jakobsen, P.K., Ribergaard, M.H., Quadfasel, D., Schmith, T., and Hughes, C.W., 2003. The near surface circulation in the Northern North Atlantic as inferred from Lagrangian drifters: variability from the mesoscale to interannual. *Journal of Geophysical Research* **108**, C8, 3251, doi:10.1029/2002JC001554.

Jónsson, S., and Brein, J., 2003. Flow of Atlantic Water west of Iceland and onto the north Icelandic Shelf. *ICES Marine Science Symposia* **219**, 326–328.

Kalnay, E., Kanamitsu, M., Kister, R., Collings, W., Deaven, D., Gandin, L., Iredell, M., Saha, S., White, G., Woollen, J., Zhu, Y., Chelliah, M., Ebisuzaki, W., Higgins, W., Janowiak, J., Mo, K.C., Ropelewski, C., Wang, J., Leetmaa, A., Reynolds, R., Jenne, R., and Joseph, D., 1996. The NCEP/NCAR 40-year reanalysis project. *Bulletin of American Meteorological Society* **77**, 437–471.

Kristmannsson, S.S, 1998. Flow of Atlantic Water into the northern Icelandic shelf area, 1985–1989. *ICES Cooperative Research Report* **225**, 124–135.

Levitus, S., and Boyer, T.P., 1994. *World Ocean Atlas 1994 Volume 4: Temperature*. NOAA Atlas NESDIS 4, Washington, D.C.

Levitus, S., Burgett, R., and Boyer, T.P., 1994. *World Ocean Atlas 1994 Volume 3: Salinity*. NOAA Atlas NESDIS 3, Washington, D.C.

McDougall, T., and Dewar, W.K., 1998. Vertical mixing and cabbeling in layered models. *Journal of Physical Oceanography* **28**, 1458–1480.

Mortensen, J., Buch, E., Kristmannsson, S.S., and Malmberg, S.A., 1991. Geostrophic velocities and volume transport calculations in the western Icelandic Sea, 1987–1990. *GSP Internal Report* **49**, Royal Danish Administration of Navigation and Hydrography and Marine Research Institute, Reykjavik, **26**.

Nilsen, J.E.Ø., Gao, Y., Drange, H., Furevik, T., and Bentsen, M., 2003. Simulated North Atlantic-Nordic Seas water exchanges in an isopycnic coordinate OGCM. *Geophysical Research Letters* **30 (10)**, 1536, doi:10.1029/2002GL016597.

Olafson, J., 2003. Winter mixed layer nutrients in the Irminger and Iceland Seas, 1990–2000. *ICES Marine Science Symposia* **219**, 329–332.

Pickart, R.S., Spall, M.A., Ribergaard, M.H., Moore, G.W.K. and Milliff, R.F., 2003a. Deep convection in the Irminger Sea forced by the Greenland tip jet. *Nature*, **424**, 152-156.

Pickart, R.S., Straneo, F., and Moore, G.W.K., 2003b. Is Labrador Sea Water formed in the Irminger Basin? *Deep Sea Research I* **50**, 23–52.

Rätz, H.-J., 1999. Structures and changes of the demersal fish assemblage off Greenland, 1982–1996. *NAFO Scientific Council Studies* **32**, 1–15.

Ribergaard, M.H., and Buch, E., 2004. Oceanographic Investigations off West Greenland 2003. *NAFO Scientific Council Research Documents* **04/001**.

Ribergaard, M.H., and Sandø, A.B., 2004. Modelling transport of cod eggs and larvae from Iceland to Greenland waters for the period 1948–2001. *In preparation*.

Rosenørn S., Fabricius, J., Buch, E., and Horsted, S.A., 1985. Record-hard winters at West Greenland. *NAFO Scientific Council Research Document* **85/061**

Schmith, T. and Hansen, C., 2003. Fram Strait Ice Export during the Nineteenth and Twentieth Centuries Reconstructed from a Multiyear Sea Ice Index from Southwestern Greenland. *Journal of Climate* **16**, 2782–2791.

Smith, P.C., 1976. Baroclinic instability in the Denmark Strait Overflow. *Journal of Physical Oceanography* **6**, 355–371.

Steele, M.; Morfley, R., and Ermold, W., 2001. PHC: A global ocean hydrography with a high quality Arctic Ocean. *Journal of Climate* **14**, 2079–2087.

Stephens, C., J. I. Antonov, T. P. Boyer, M. E. Conkright, R. A. Locarnini, T. D. O'Brien, and H. E. Garcia, 2002, *World Ocean Atlas 2001 Volume 1: Temperatur*e, S. Levitus, Ed., NOAA Atlas NESDIS 49, U. S. Government Printing Office, Washington, D. C., 176 pp.

Walsh J.E., 1978. A data set on Northern Hemisphere sea ice extent. World Data Center-A for Glaciology (Snow and Ice). *Glaciological Data, Report GD-2*, part 1, 49–51.
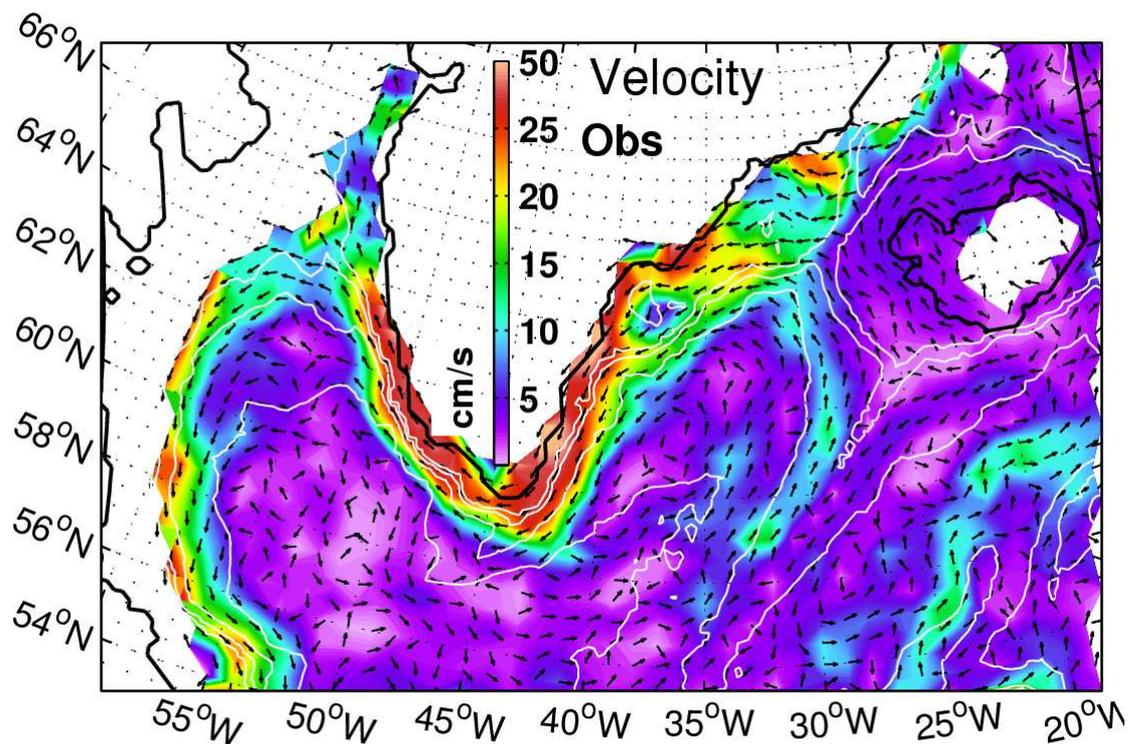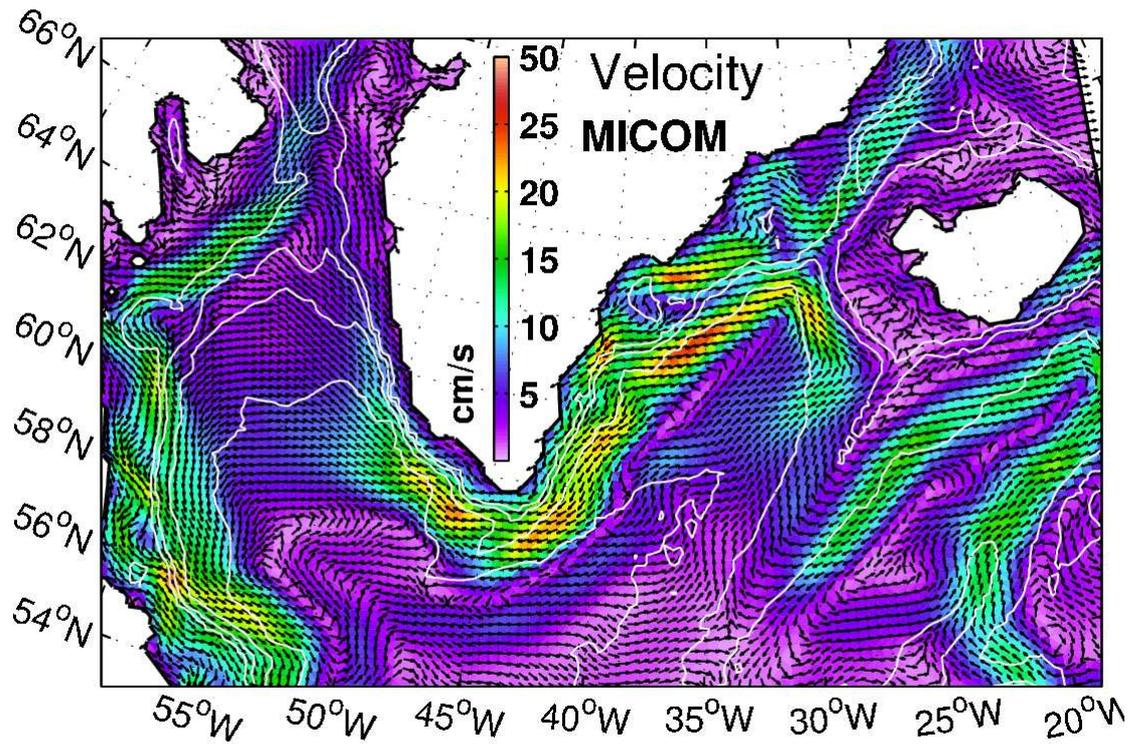
Figure 1. Mean surface velocity for MICOM (top) and from surface drifters (bottom). The MICOM surface velocities are the mean mixed layer velocities for the period 1948–2001, while the drifter velocities are deduced from surface drifters drogued at 15 m depth for the 1990s. Coloured contours are velocities in cm/s and the arrows the direction of the current. Note velocity scale change at 25 cm/s. The black lines mark the model domain, and the white contours are model bathymetry: 500, 1000, 2000, 3000 m.
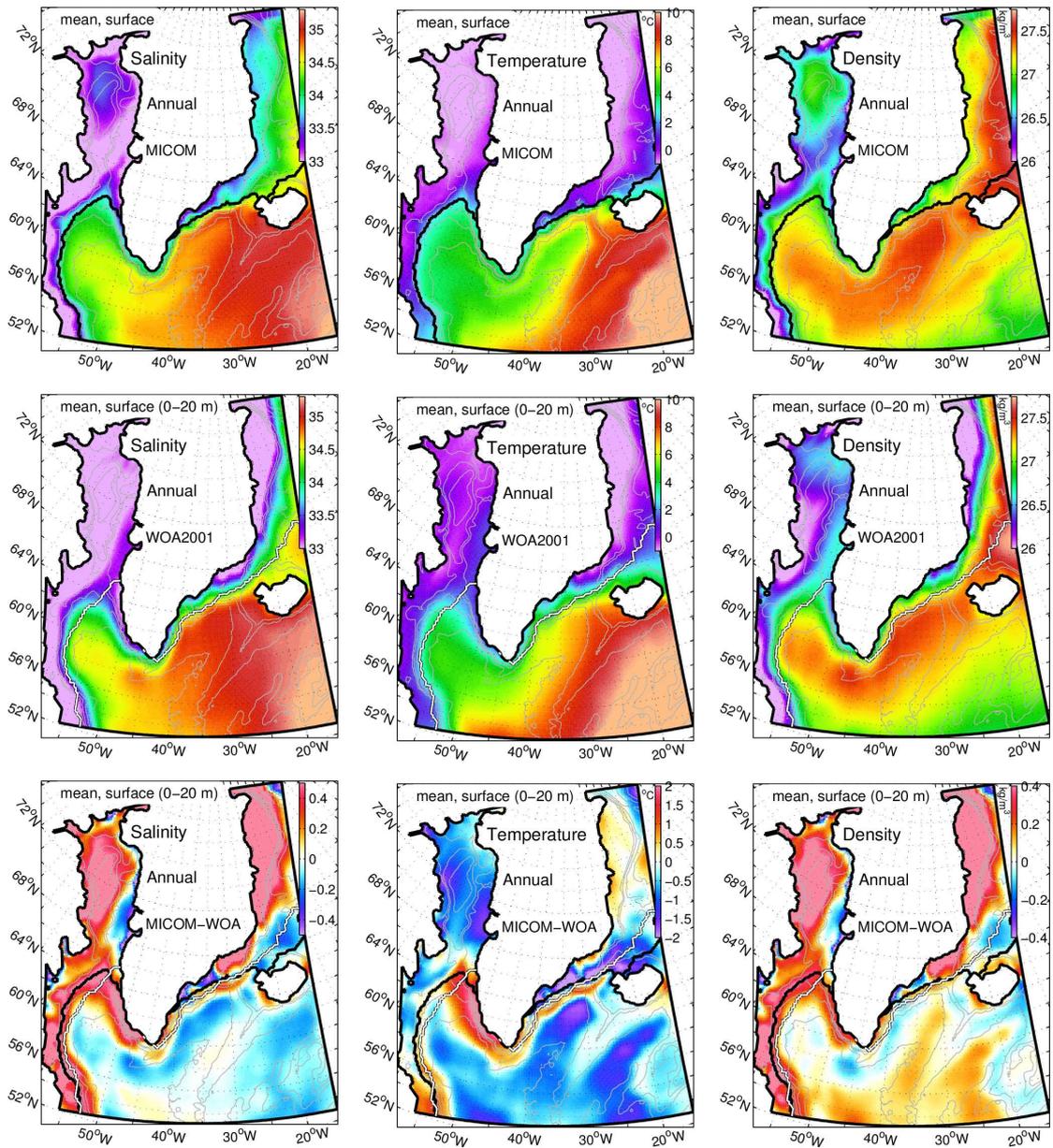
Figure 2. Annual mean surface salinity (left), surface temperature (middle) and surface density (right) for MICOM (top), WOA (middle) and MICOM minus WOA (bottom). Thick black line is model ice edge and thick white line is the Walsh and Chapman ice edge. The surface layer shown is the surface mixed layer for MICOM and 0–20 m for WOA. Depth contours are model depths at 500, 1000, 2000 and 3000 m.
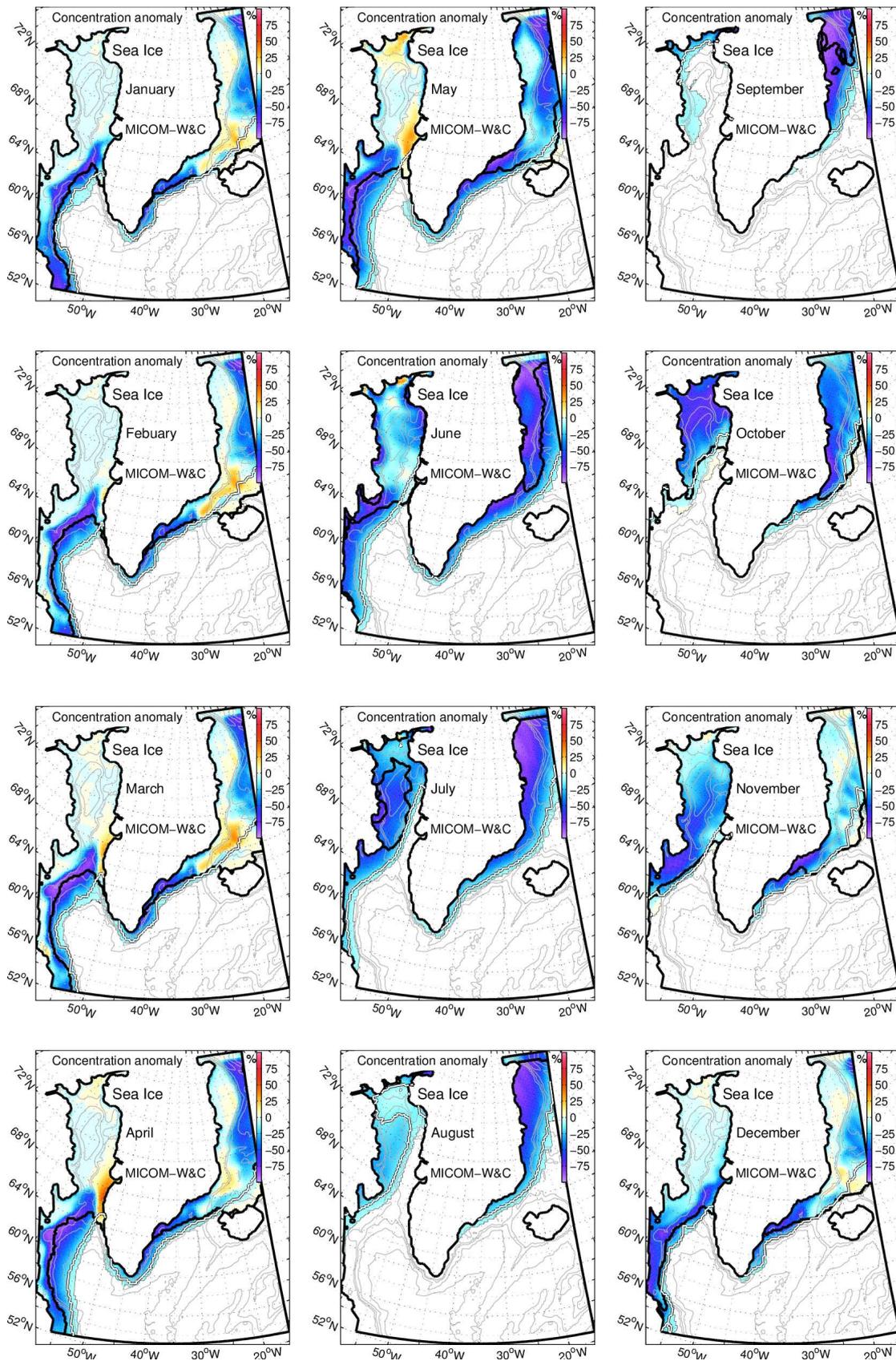
Figure 3. MICOM minus Walsh and Chapman sea-ice concentration (see text for details). Black and white thick lines represent the ice-edge for "normal" years in MICOM and the Walsh and Chapman climatology (see text for more info). Model depth contours are 500, 1000, 2000, 3000 m.
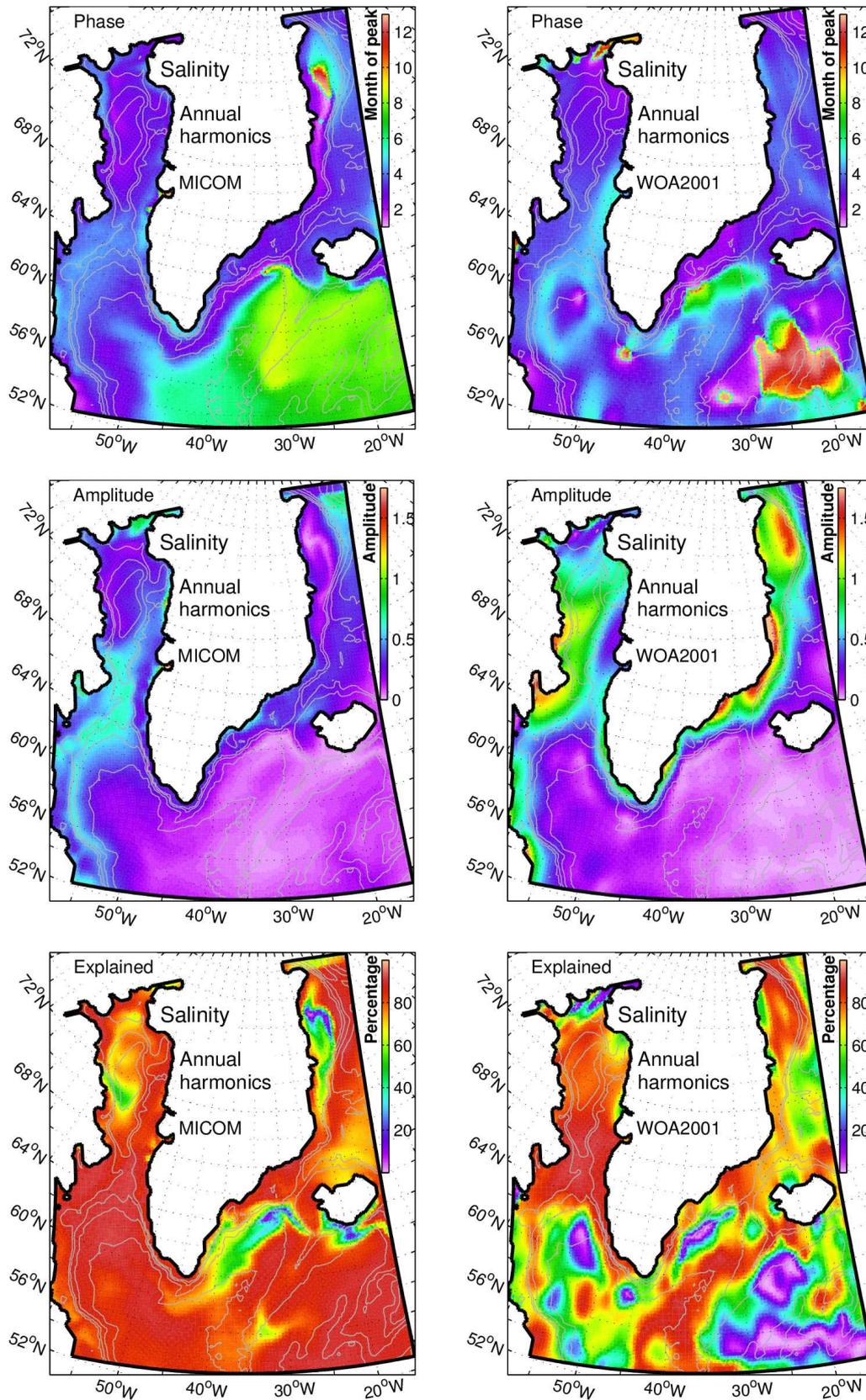
Figure 4a. Annual harmonics for surface salinity for MICOM (left) and from WOA (right).
From top to bottom: Distribution of phase, amplitude and explained variance.
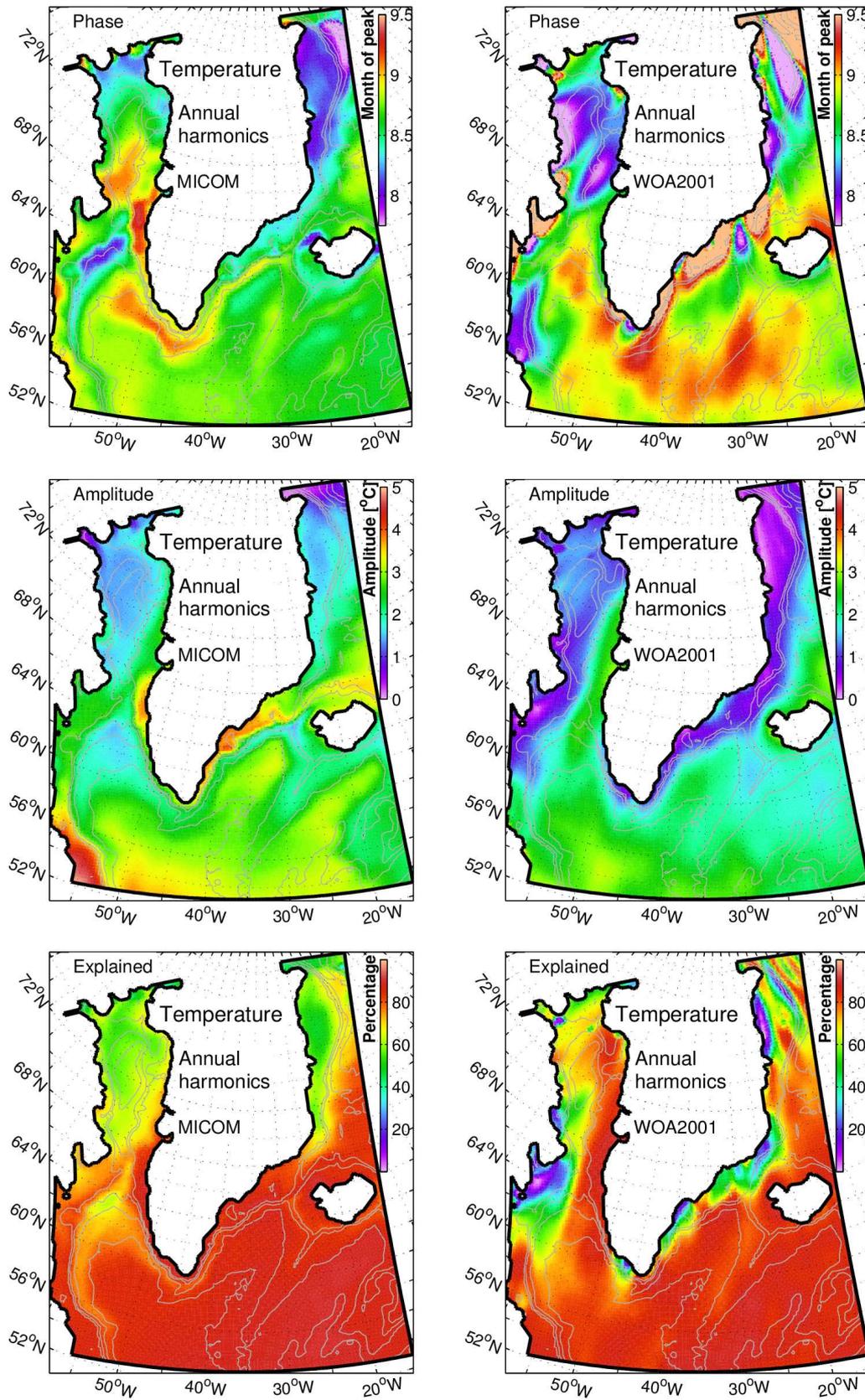
Figure 4b. As Figure 4a but for potential temperature.
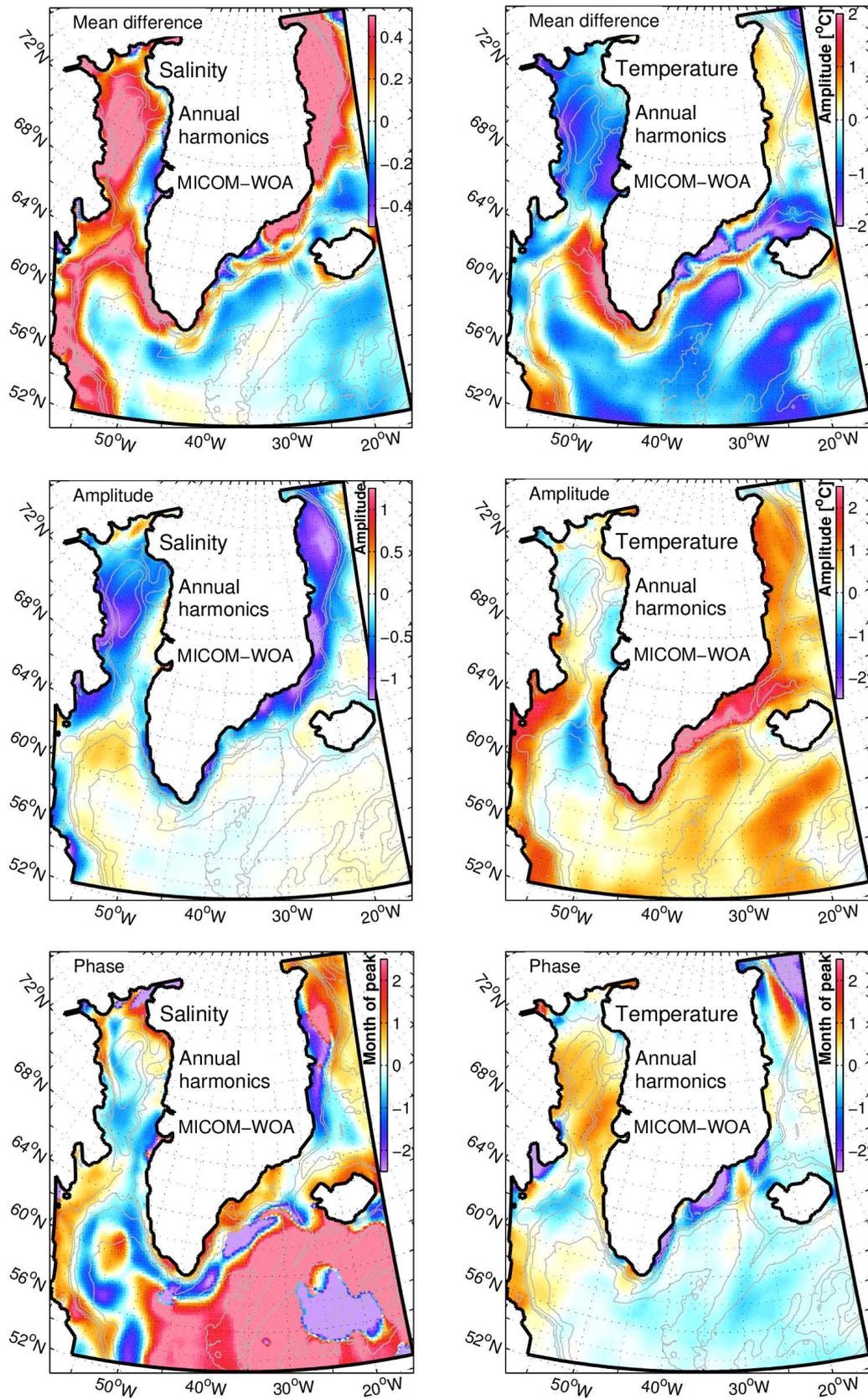
Figure 5. Difference in the calculated annual harmonics for MICOM and WOA surface salinity (left) and temperature (right). From top to bottom: Annual mean difference, difference in amplitude and phase difference. Bottom contours shown: 500, 1000, 2000, 3000 m.
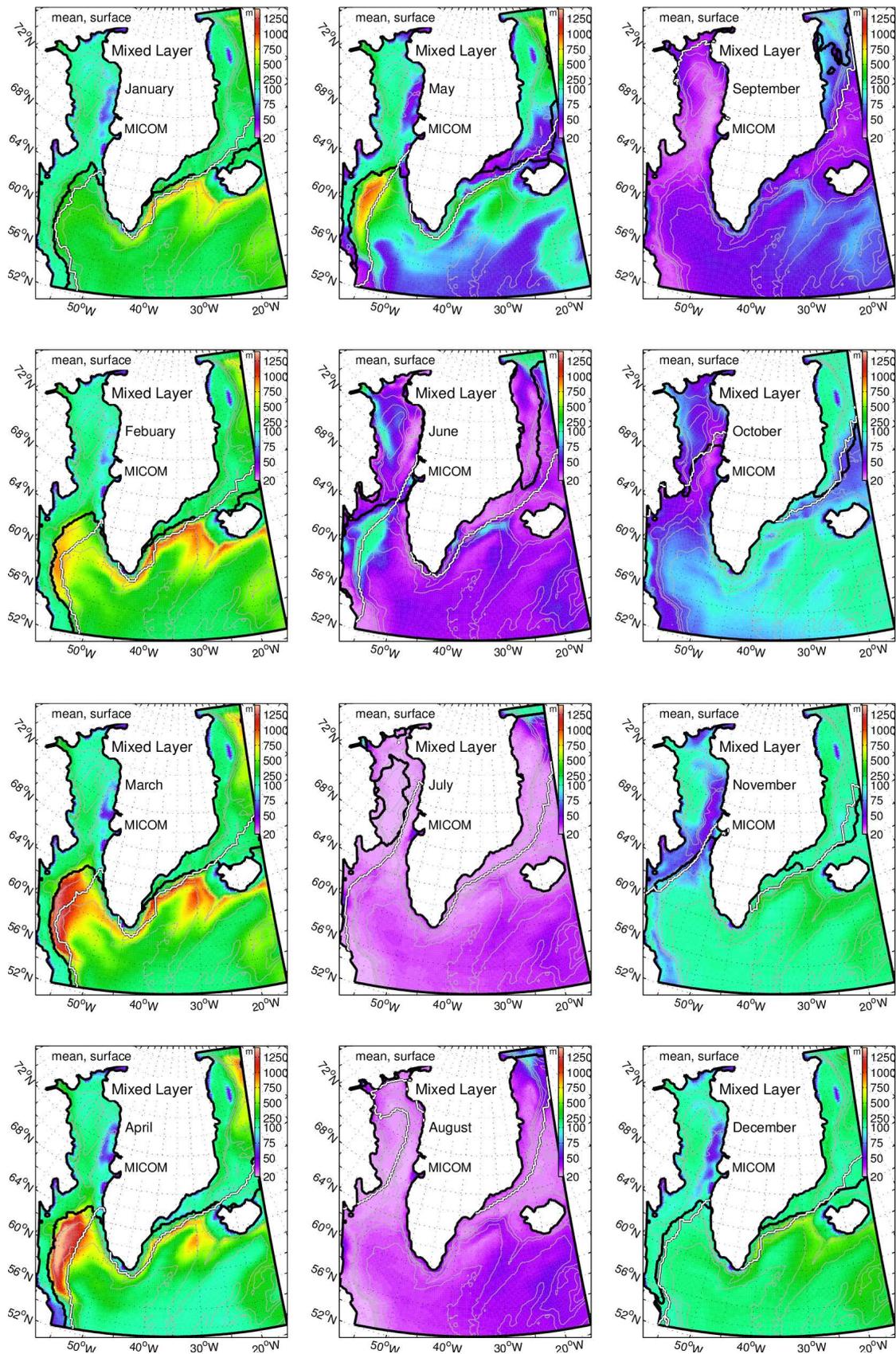
Figure 6a. Monthly mean mixed layer depths (colours) and maximum sea-ice extent (Thick solid black line) in MICOM. Note the colorbar change resolution at 100 m. Thick white line is the Walsh and Chapman ice-edge climatology (see text for details). Model depth contours are 500, 1000, 2000, 3000 m.
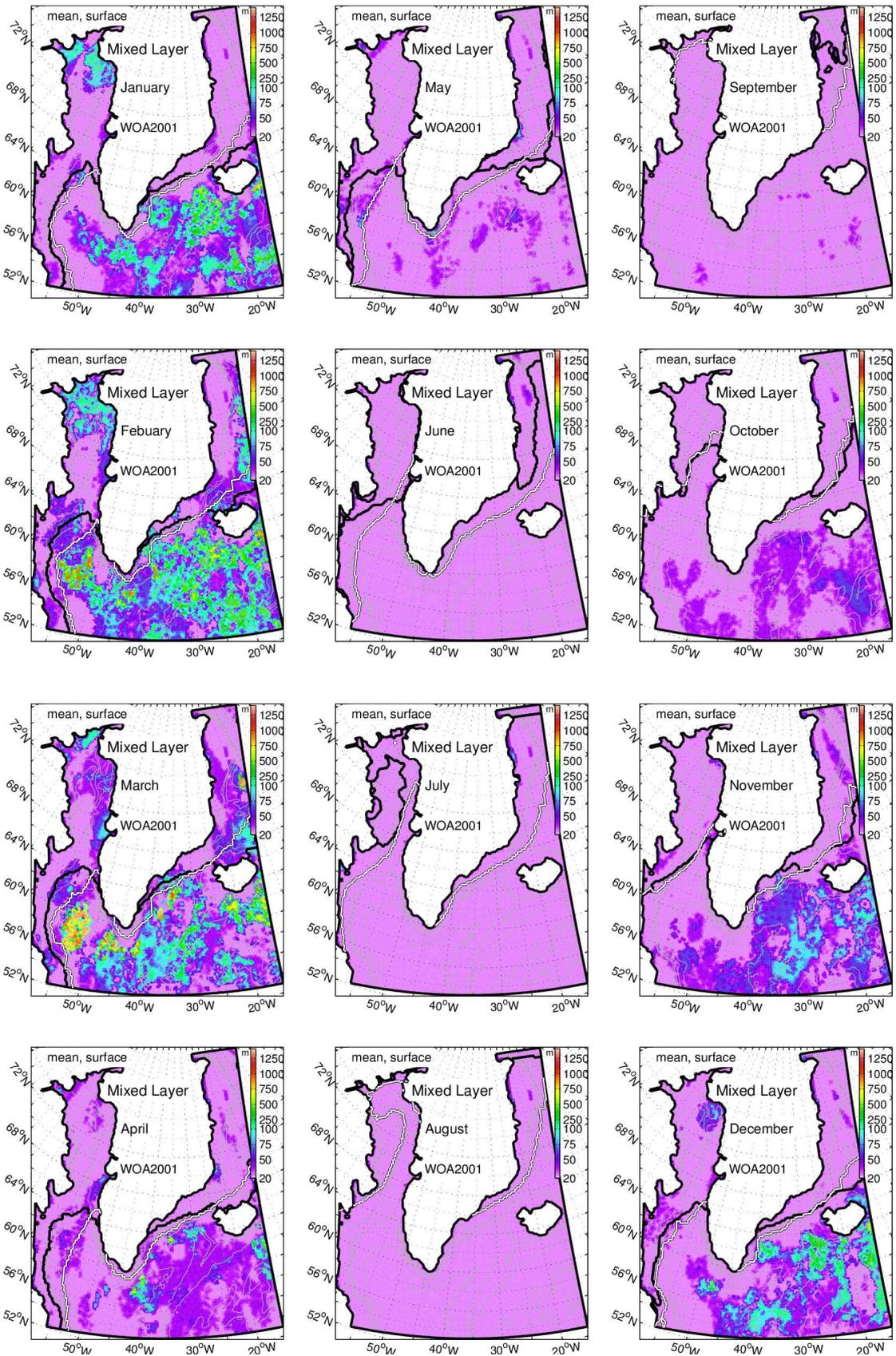
Figure 6b. As Figure 6a but for WOA.
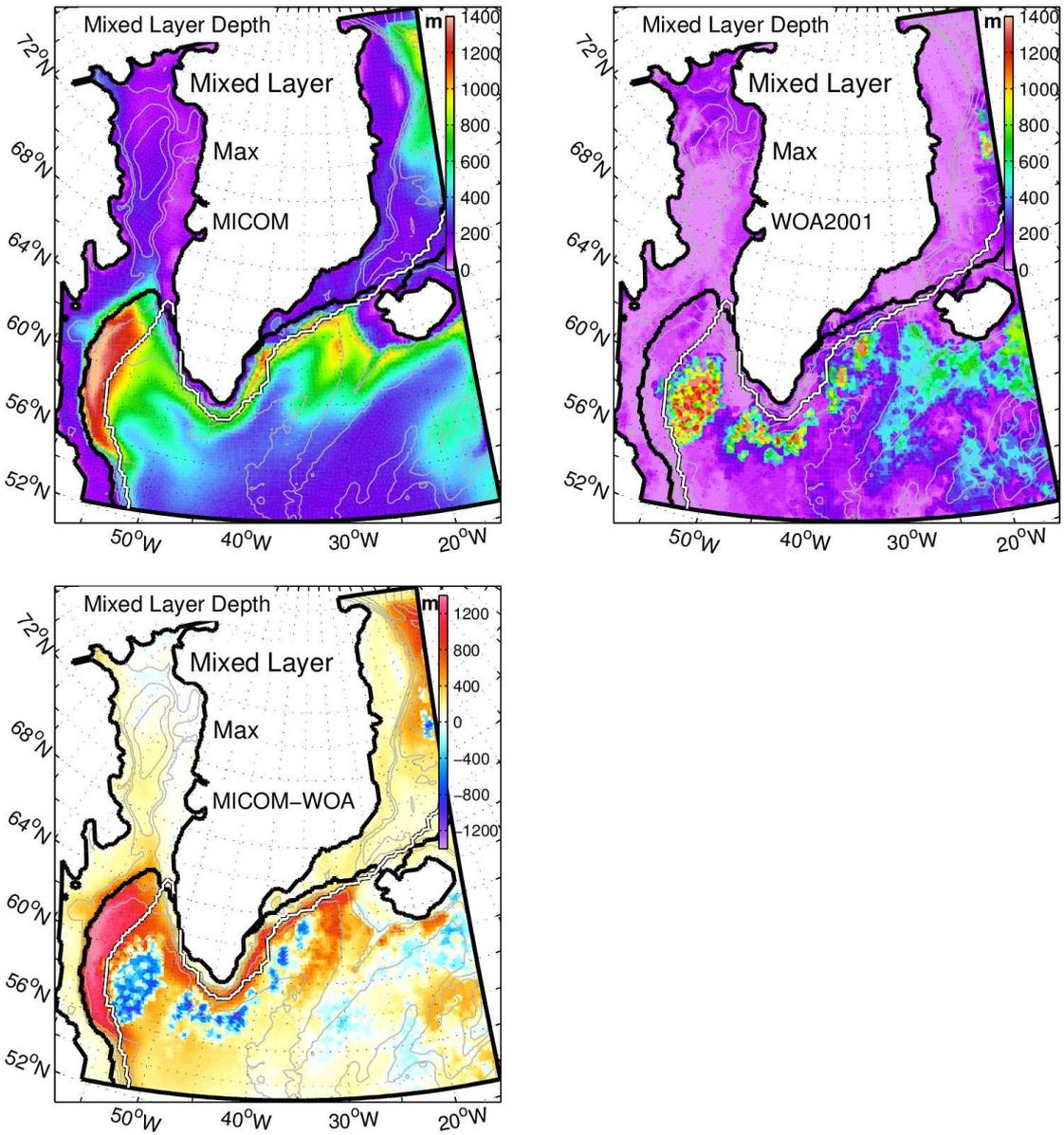
Figure 7. Top: maximum mixed layer depth from MICOM and WOA. Bottom: MICOM less WOA maximum mixed layer depth. Black line is the model ice-edge and white line is the annual Walsh and Chapman ice-edge at its maximum.
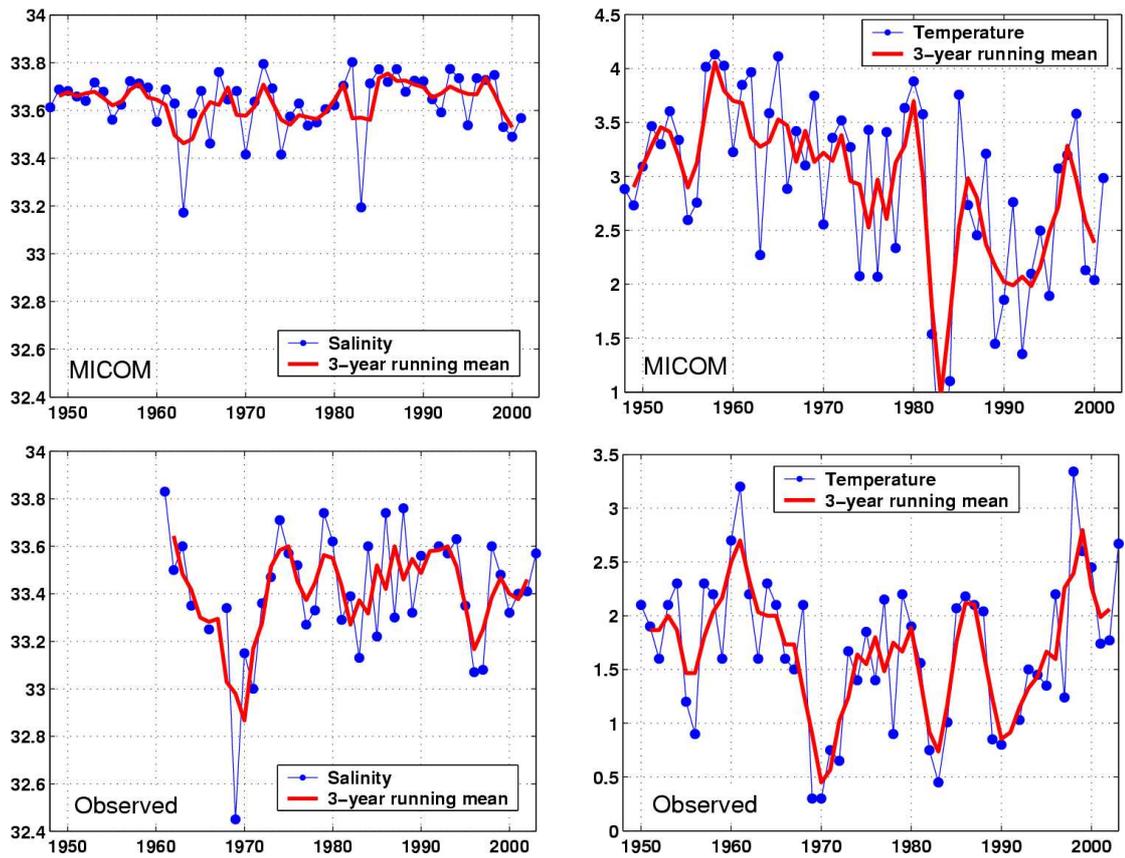
Figure 8. Modelled (top) and observed (bottom) salinity (left) and potential temperature [°C] (right) at Fylla Bank station 2. Note different scale on temperature, but same span. Thick lines are 3-years running means.
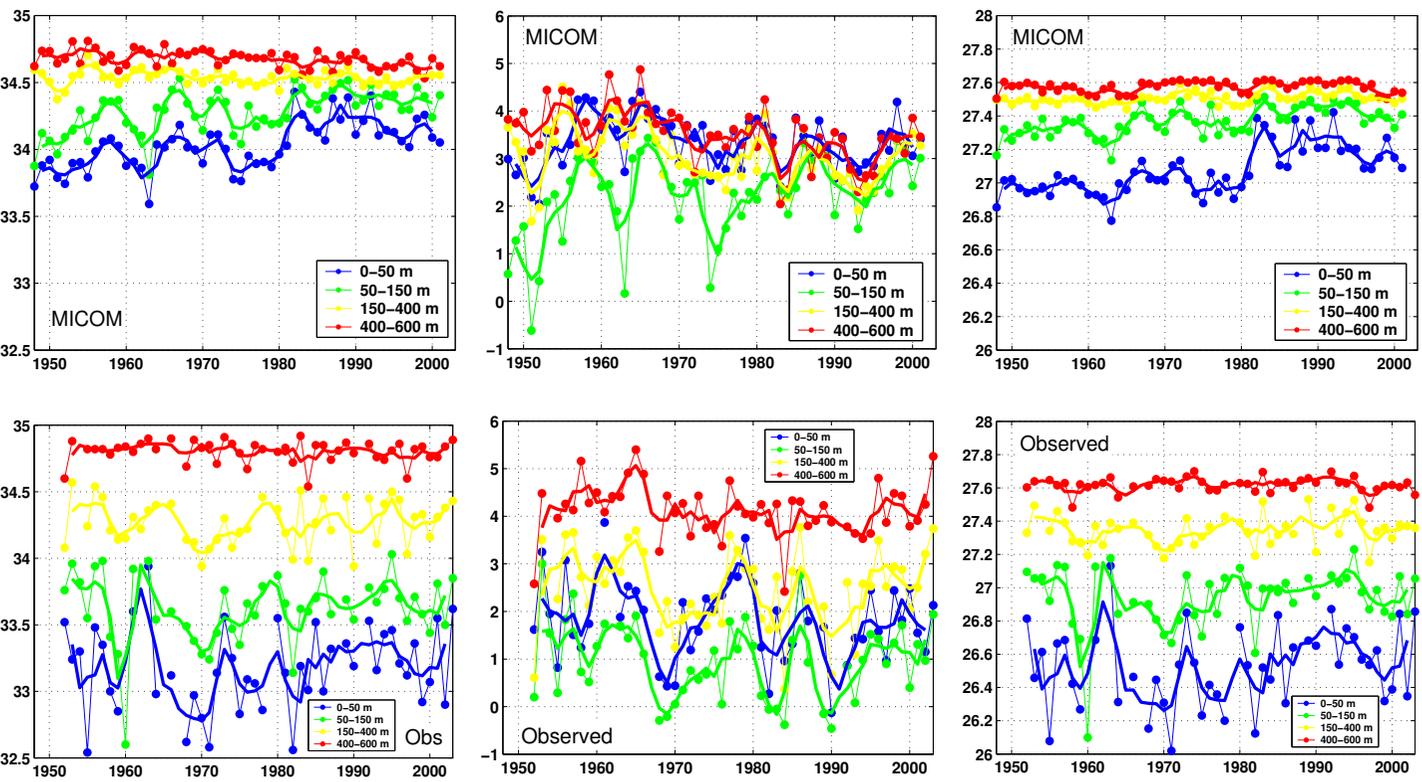
Figure 9. Modelled (top) and observed (bottom) salinity (left), potential temperature [°C] (middle) and potential density [kg/m³] (right) at Fylla Bank station 4. Mean values for four different depth intervals are shown: 0–50 m, 50–150 m, 150–400 m, 400–600 m. Thick lines are 3-years running means.
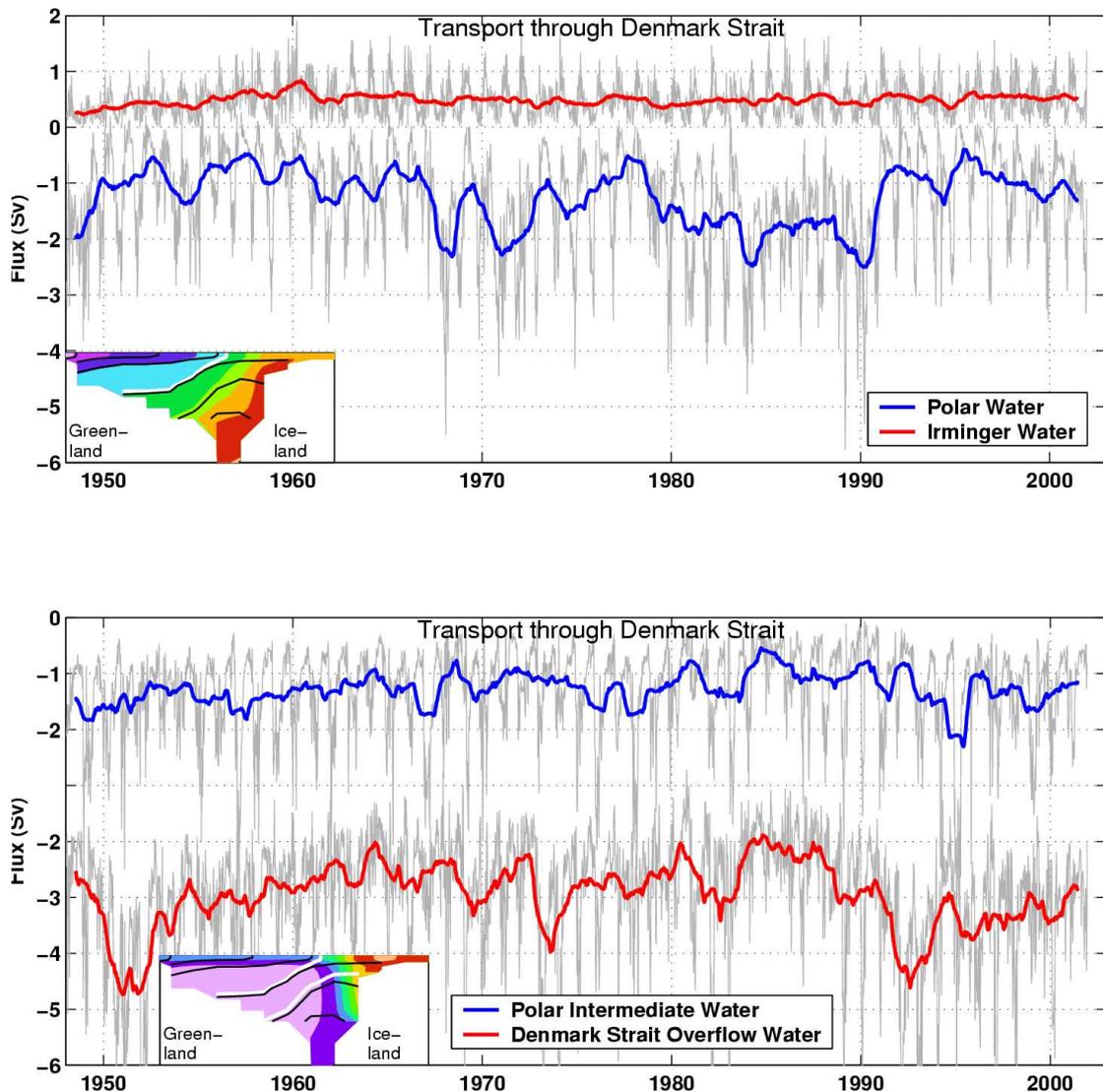
Figure 10. Transport through Denmark Strait calculated from the model MICOM for the period 1948–2001. Top: Red is the 1-year running mean transport within the North Icelandic Irminger Current here defined as positive normal transport (1 Sv = 1 Sverdrup = 10^6 m^3/s). Blue is the transport within the East Greenland Current defined by salinities below 34. Gray is the weekly mean transport. Inlay shows the cross section of the Denmark Strait. Colours are model mean (1948–2001) salinity with an interval of 0.2. White thick line is 34. Black lines are model density. The depth interval shown is 0–500 m and the strait is 388 km wide. Bottom: As top but for Polar Intermediate Water (PIW) and Denmark Strait Overflow Water (DSOW). Contours in the inlay are Potential temperature from -1°C to 5°C. Tick white lines are salinity line 34 and density line 27.55 kg/m^3. PIW is defined between these lines and DSOW is defined as densities above 27.55 kg/m^3. See text for further explanation for these alternative definitions.